Supporting Information For: Correlating Broadband Photoluminescence with Structural Dynamics in Layered Hybrid Halide Perovskites

Alexandra A. Koegel,[†] Eve M. Mozur,[†] Iain W. H. Oswald,[†] Niina H. Jalarvo,[‡] Timothy R. Prisk,[¶,‖] Madhusudan Tyagi,[¶,§] and James R. Neilson[*,†]

†*Colorado State University, Department of Chemistry, Fort Collins, Colorado 80523-1872, United States*

‡*Neutron Scattering Division, Oak Ridge National Laboratory, Oak Ridge, Tennessee 37831, United States*

¶*NIST Center for Neutron Research National Institute of Standards and Technology, Gaithersburg, Maryland 20899, United States*

§*Department of Materials Science and Engineering, University of Maryland, College Park, Maryland 20742, United States*

‖*Present address: Division of Chemistry and Chemical Engineering, California Institute of Technology, Pasadena, California 91125, United States.*

E-mail: james.neilson@colostate.edu

Supplemental Information

Preliminary Characterization

For the compounds synthesized in this study, PXRD data were modeled with space groups of *Pbca* for $(n\text{BA})_2\text{PbBr}_4$, $P2_1/c$ for $(\text{ODA})\text{PbBr}_4$, and $P2_1/c$ for $(\text{GABA})_2\text{PbBr}_4$ using previously reported structures[1] with the Rietveld method implemented in TOPAS v6 (Bruker AXS). The room temperature photoluminescence spectroscopy reveals emission peaked near 415 nm (Figure S2), in agreement with a previous study.[1]

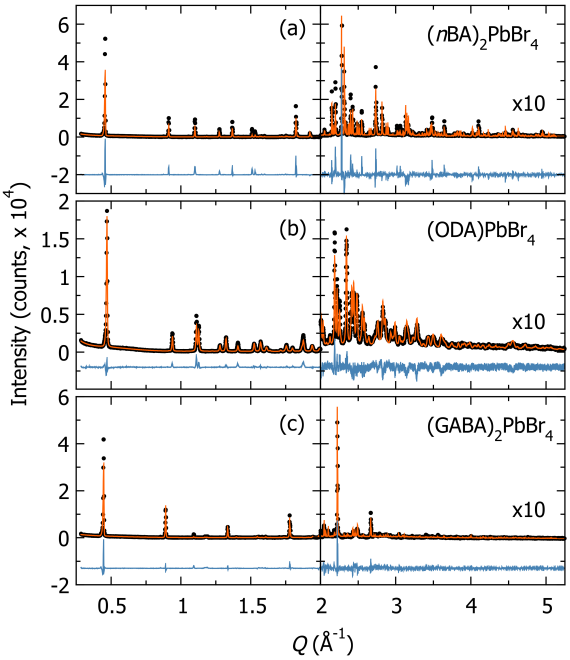

Figure S1: Powder X-ray diffraction of (a) $(n\text{BA})_2\text{PbBr}_4$, (b) $(\text{ODA})\text{PbBr}_4$, and (c) $(\text{GABA})_2\text{PbBr}_4$. Black circles, orange line, and blue line represent the data, Rietveld refinement, and difference curve, respectively.

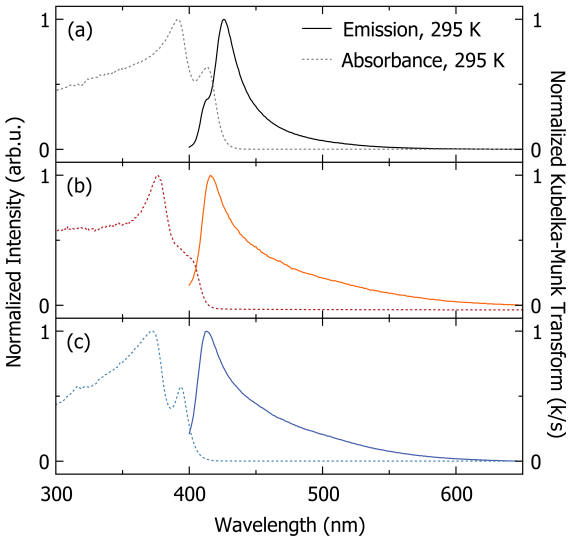

Figure S2: Ambient temperature (295 K) normalized photoluminescence intensity with excitation at 375 nm (solid lines, left axis) showing narrow emission centered at 415 nm and Kubelka-Munk transform (k/s) (dotted lines, right axis) of (a) $(n\text{BA})_2\text{PbBr}_4$ (black), (b) $(\text{ODA})\text{PbBr}_4$ (red), and (c) $(\text{GABA})_2\text{PbBr}_4$ (blue).

Thermal activation of motion

Activation energies vary by molecule and motion occurring within $(n\text{BA})_2\text{PbBr}_4$, $(\text{ODA})\text{PbBr}_4$, and $(\text{GABA})_2\text{PbBr}_4$. The organic cation dynamics do not follow classically Arrhenius behavior as seen in Figure S3. The data presented as $\ln(\tau)$ v. T^{-1} are not linear and there are multiple relaxation times observed at $T \geq 275$ K for $(n\text{BA})_2\text{PbBr}_4$ and $T \geq 275$ K for $(\text{ODA})\text{PbBr}_4$.

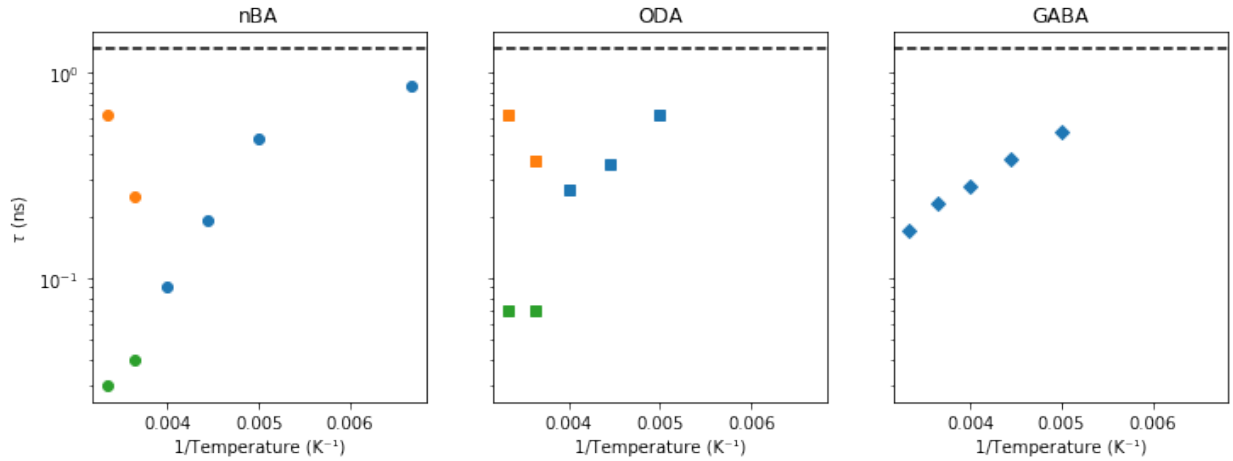

Figure S3: ln(τ) vs. T^{-1} (left) $(n\text{BA})_2\text{PbBr}_4$, (middle) $(\text{ODA})\text{PbBr}_4$, and (right) $(\text{GABA})_2\text{PbBr}_4$ calculated from QENS data collected from 150 K to 300 K. Blue symbols indicate a singular Lorentzian. Orange and green symbols indicate two separate Lorentzian functions used to model the QENS data.

Quasi-elastic scattering from $(n\text{BA})_2\text{PbBr}_4$, $(\text{ODA})\text{PbBr}_4$, and $(\text{GABA})_2\text{PbBr}_4$

There is no QENS observed at liquid nitrogen temperatures (Figure S4). This lack of resolvable QENS is due to the speed of the organic cation motions occurring within the broad elastic line at low temperatures, making quasi-elastic interactions unobservable within the resolution of the instrument. At temperatures $<$ 200 K only the motions of *n*BA are observable and have a full width at half maximum (FWHM) of roughly 1.5 μeV (Figures S5 and S6).

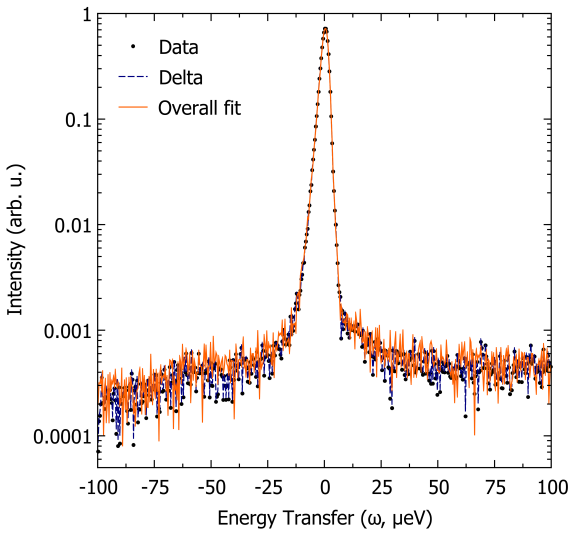

Figure S4: Representative QENS spectra of $(GABA)_2PbBr_4$ at $T = 77$ K for $Q = 1.1$ Å^{-1} collected at BASIS. The spectra are shown as black circles, with the overall fit shown as a solid red line. The data are modeled with a δ-function convolved with an instrument resolution function collected for each sample at $T = 20$ K to account for elastic scattering, shown here as a blue dashed line. There are no quasi-elastic interactions present.

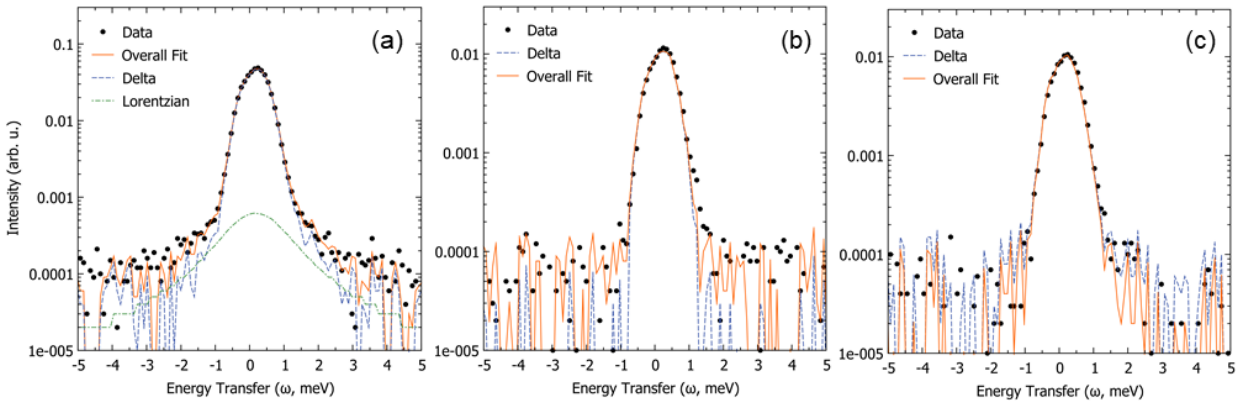

Figure S5: Quasi-elastic neutron scattering at 150 K for (a) $(n\text{BA})_2PbBr_4$ (b) $(ODA)PbBr_4$, and (c) $(GABA)_2PbBr_4$ collected at HFBS. The representative spectra are shown as black circles, with the overall fit shown as a solid red line. The data are modeled with a δ-function convolved with an instrument resolution function collected for each sample with a vanadium standard to account for elastic scattering, shown here as a blue dashed line. The broadening from quasi-elastic scattering is fit with a Lorentzian, shown as a green dash-dotted lines only in (a). Note the log scale on the y-axis.

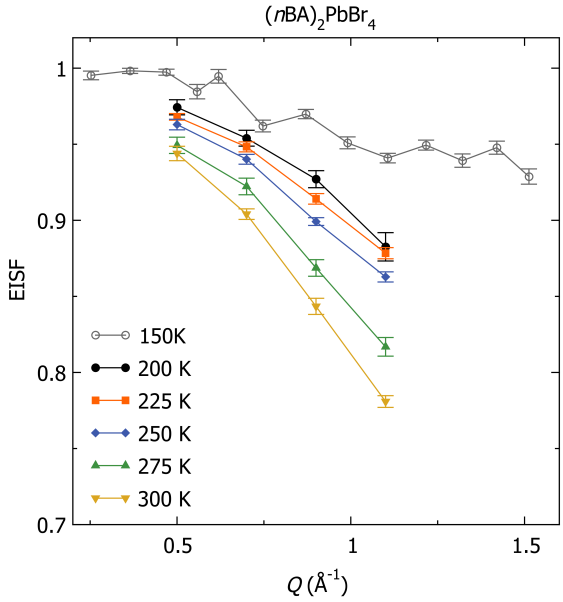

Figure S6: Elastic incoherent structure factor of $(n\text{BA})_2\text{PbBr}_4$ at 150 K to 300 K extracted from quasi-elastic neutron scattering data from HFBS (150 K) and BASIS (200 K to 300 K). Error bars represent one standard deviation.

Rotational mode analysis of $(n\text{BA})_2\text{PbBr}_4$, $(\text{ODA})\text{PbBr}_4$, and $(\text{GABA})_2\text{PbBr}_4$

Figures S8 and S9 are the molecules with either a total model (Figure S8) or C_3 model (Figure S9) applied to the data at temperatures 200 K to 300 K. Figure S8a shows the full model for $(n\text{BA})_2\text{PbBr}_4$ that includes $C_2 \otimes C_3$ of the $-\text{NH}_3$ headgroup (a C_2 of the $-\text{CH}_2$ adjacent to the $-\text{NH}_3$ terminal group with a C_3 of the ammonium headgroup), a C_3 of the methyl group, and librations of the aliphatic hydrogens applied to the data at all temperatures, as depicted in Figure S7. The model describes the data at 300 K and does not describe the data for $T \leq 275$ K. When the model is reduced to describe only the C_3 motions of the ammonium headgroup and methyl group, the model fits the data at 275 K (Figure S9). All other data has an EISF representative of a more static molecule than a C_3 model implies. Therefore, fractional motion was applied to fit data for $T < 275$ K. The best fit parameters for fractional C_3 motion are tabulated in Table S2 and plotted in Figure S10.

Figure S8b shows the results from fitting the full dynamic model for ODA in $(\text{ODA})\text{PbBr}_4$ that includes $C_2 \otimes C_3$ of the $-\text{CH}_2\text{NH}_3$ headgroup in conjunction with a C_2 of the $-\text{CH}_2$ adjacent

to the $-NH_3$ terminal group and librations of the aliphatic hydrogens applied to the data at all temperatures depicted in Figure S7. This model only describes the data for $T \geq 275$ K. However, when the model is changed to only describe the C_3 motion of the ammonium head groups, it is a good fit to data T = 250 K, whereas the EISFs at $T \leq 225$ K describe a more static molecule than the model. Therefore, fractional motion was applied to fit the low temperature data. The best fit parameters for fractional C_3 motion are tabulated in Table S2 and plotted in Figure S10.

Figure S8c shows the full model for $(GABA)_2PbBr_4$ that includes $C_2 \otimes C_3$ of the $-CH_2NH_3$ headgroup in conjunction with a C_2 of the $-CH_2$ adjacent to the $-NH_3$ terminal group and $-COOH$ group, and librations of the aliphatic hydrogens applied to the data at all temperatures depicted in Figure S7. This model does not describe any of the data. When the motion is reduced to a model describing only C_3 motions, the data at T = 300 K fits well; however, none of the other temperatures are described. Therefore, a fractional C_3 model was applied. The best fit parameters for fractional C_3 motion are tabulated in Table S2 and plotted in Figure S10.

Relaxation times of the principle hopping motions of the cations described above are listed in Table S1 and shown in Figure S11. Extrapolated relaxation times were calculated with a least squares polynomial fit in Python. The *n*BA cations have the shortest measured relaxation times at all temperatures except 77 K, where GABA has the shortest extrapolated relaxation time.

Table S1: Relaxation times of hydrogen motions (τ, ns) extracted from QENS spectra. Error bars represent one standard deviation.

	Relaxation times† (ns)		
Temp (K)	*n*BA	ODA	GABA
77	5.35*	4.59*	1.94*
150	0.86±0.1	1.36*	0.876*
200	0.48±0.02	0.62±0.009	0.52±0.05
225	0.19±0.004	0.36±0.009	0.38±0.02
250	0.09±0.002	0.27±0.004	0.28±0.01
275	0.25±0.07, 0.04±0.005	0.37±0.02, 0.07±0.003	0.23±0.005
300	0.62±0.27, 0.03±0.0008	0.62±0.07, 0.07±0.0007	0.17±0.005

† Calculated with the formula: $\mathrm{HWHM}_{\mathrm{Lorentzian}} = \hbar/\tau$

* Estimated extrapolated relaxation time values. Values were extrapolated assuming $\ln(\tau) = AT + B$, fitting A and B across the temperatures for which a single tau is recorded. (Figure S11). Uncertainty calculated for *n*BA at 150 K used error propagation of one Q-group from DAVE.

Table S2: Best fit parameters for hydrogens undergoing fractional C_3 motion in $(n\text{BA})_2\text{PbBr}_4$, $(\text{ODA})\text{PbBr}_4$, and $(\text{GABA})_2\text{PbBr}_4$. Errors were estimated from taking the square root of the diagonals of the covariance matrix.

C_3 Fraction			
Temperature (K)	*n*BA	ODA	GABA
200	0.60(2)	0.6000(6)	0.2000(3)
225	0.70(1)	0.9000(3)	0.4000(2)
250	0.80(1)	-	0.53000(4)
275	-	-	0.7000(8)
300	-	-	0.9000(7)

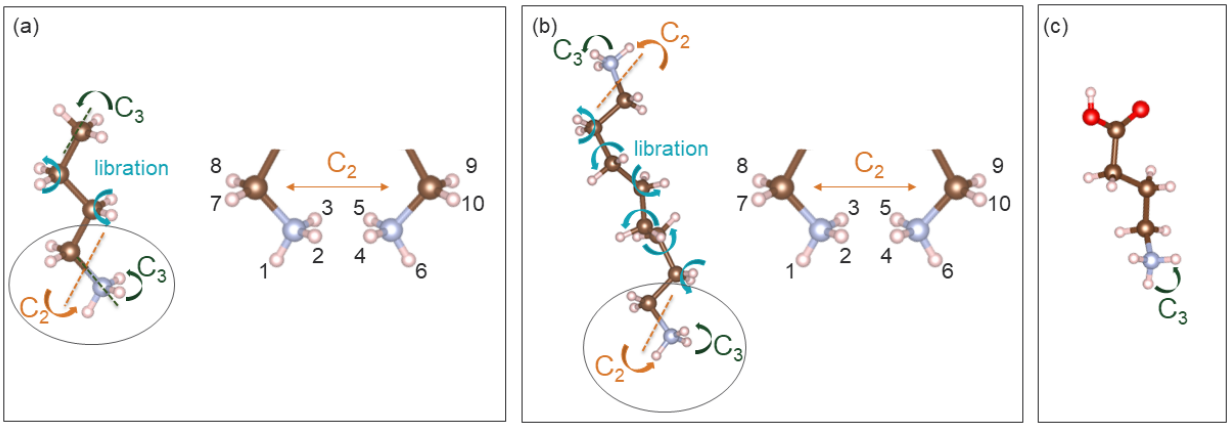

Figure S7: Visualization of rotational motions simulated in jump models in (a) $(n\text{BA})_2\text{PbBr}_4$, (b) $(\text{ODA})\text{PbBr}_4$, and (c) $(\text{GABA})_2\text{PbBr}_4$ at room temperature. Green arrows indicate C_3 rotations of the $-\text{NH}_3$ and CH_3 groups. Orange arrows indicate a C_2 rotation of the $-\text{CH}_2\text{NH}_3$ head group about a predetermined angle as indicated in the cartoon on the left.[2] Blue arrows indicate librations of the $-\text{CH}_2$ chain.

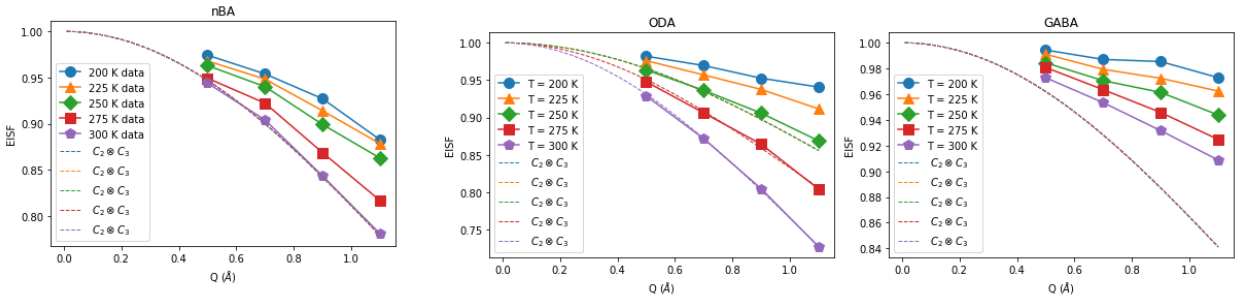

Figure S8: Elastic incoherent structure factor of (left) $(n\text{BA})_2\text{PbBr}_4$, (middle) $(\text{ODA})\text{PbBr}_4$, and (right) $(\text{GABA})_2\text{PbBr}_4$ at 200 K to 300 K extracted from QENS data at BASIS fit with a jump model labeled as $C_2 \otimes C_3$ that, depending on the molecule, includes: $C_2 \otimes C_3$ of the $-\text{CH}_2\text{NH}_3$ headgroup, C_3 of the ammonium and methyl groups, C_2 of the $-\text{CH}_2\text{CH}_3$ headgroup and $-\text{COOH}$, and librations of the CH_2 backbone, as described above. The full model does not describe all motions at all temperatures for the three molecules studied. The models for temperatures in (a) $T \leq 300$ K, (b) $T \leq 275$ K, and (c) $T \leq 300$ K are overlapping.

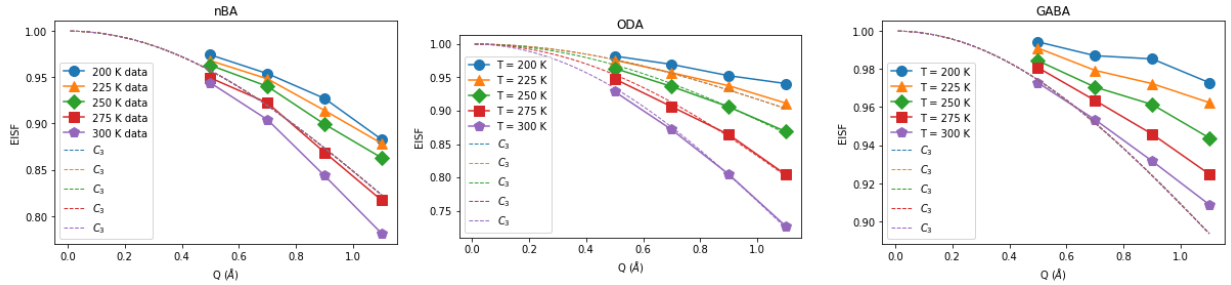

Figure S9: Elastic incoherent structure factor of (left) $(n\text{BA})_2\text{PbBr}_4$, (middle) $(\text{ODA})\text{PbBr}_4$, and (right) $(\text{GABA})_2\text{PbBr}_4$ at 200 K to 300 K extracted from QENS data at BASIS modeled by a jump model describing the C_3 rotations of the ammonium headgroup, as described in the narrative. This model does not describe all motions at all temperatures for the three molecules studied. The models for $T \leq 300$ K, (b) $T \leq 250$ K, and (c) $T \leq 300$ K are overlapping

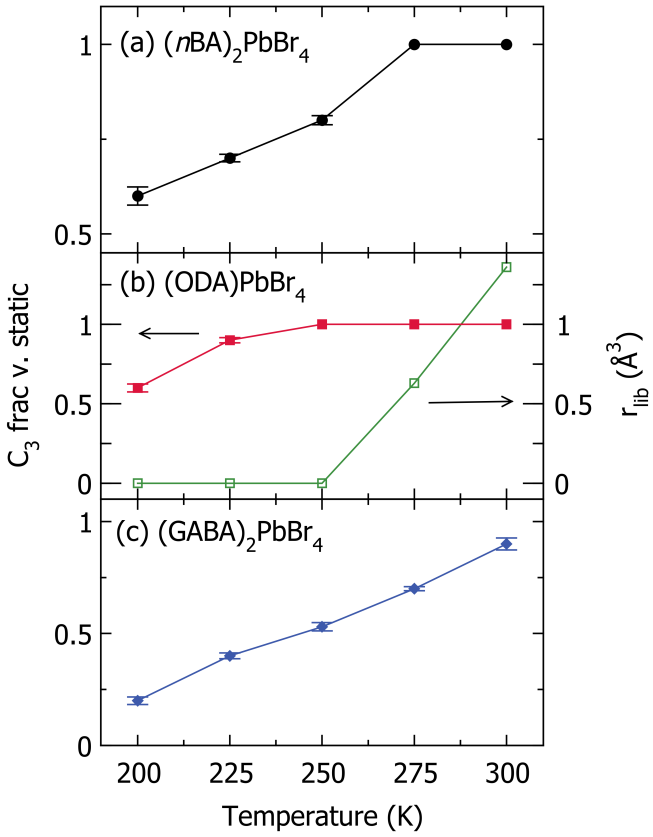

Figure S10: Fraction of C_3 motion of the organic cation in (a) $(n\text{BA})_2\text{PbBr}_4$ (black), (b) $(\text{ODA})\text{PbBr}_4$ (red), and (c) $(\text{GABA})_2\text{PbBr}_4$ (blue) at 200 K to 300 K extracted from QENS data at BASIS modeled by a jump model describing the C_3 rotations of the ammonium headgroup and methyl group, as described in the narrative. Values are listed in Table S2. (b, green) Libration radius of the of the $-\text{CH}_2-$ hydrogens in $(\text{ODA})\text{PbBr}_4$ at 200 K to 300 K extracted from QENS data at BASIS modeled by a jump model as described in the narrative. Libration radii are as follows: At T = 300 K the libration distance is 1.36 Å^{-1}, at T = 275 K the libration distance is 0.630 Å^{-1}.

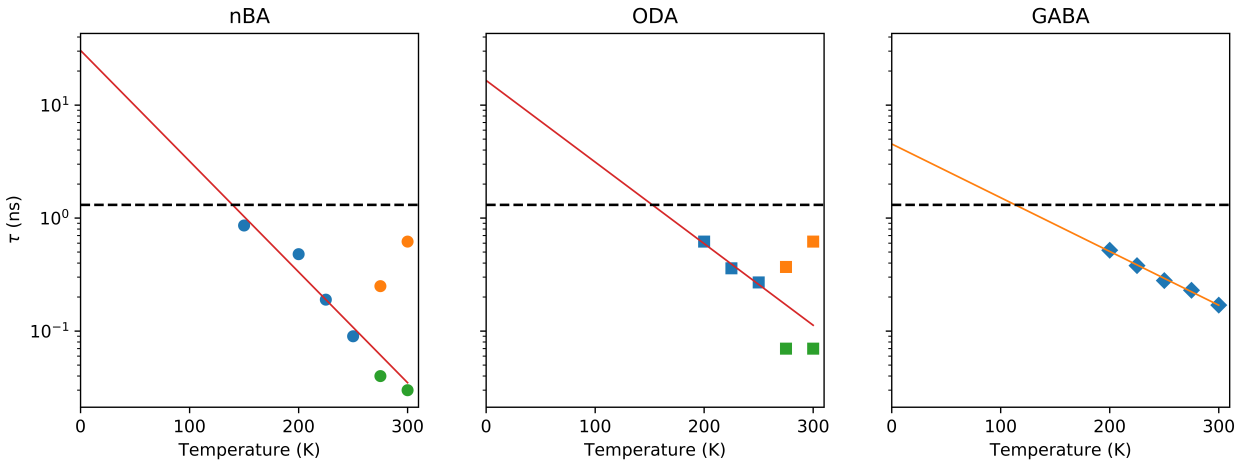

Figure S11: Extrapolated relaxation times for (left) $(n\text{BA})_2\text{PbBr}_4$, (middle) $(\text{ODA})\text{PbBr}_4$, and (right) $(\text{GABA})_2\text{PbBr}_4$. Extrapolations were done with a least squares polynomial fit in Python. Values determined from extrapolations are in Table S1. Dashed line indicates instrument resolution. Blue symbols indicate a singular Lorentzian. Orange and green symbols indicate two separate Lorentzian functions used to model the QENS data.

Table S3: *A*-site volumes (Å^3, calculated from the [NBr_8] polyhedra in VESTA as described in the narrative) determined from the 295 K crystal structures of (nBA)$_2$PbBr$_4$, (ETA)$_2$PbBr$_4$, (PEA)$_2$PbBr$_4$, (MPenDA)PbBr$_4$, (ODA)PbBr$_4$, (BDA)PbBr$_4$, (AEA)PbBr$_4$, (HIS)PbBr$_4$, and (GABA)$_2$PbBr$_4$.[1†]

Compound	Out-of-plane tilt angle (°)[1]	Volume (Å^3)	Observation of BBPL[1]
(nBA)$_2$PbBr$_4$	2.8	84.6	No
(ETA)$_2$PbBr$_4$	6.3	90.6	Yes, minimal
(PEA)$_2$PbBr$_4$	10.4	84.2	Yes
(MPenDA)PbBr$_4$	17.9	78.6	Yes
(ODA)PbBr$_4$	19.0	79.2	Yes
(BDA)PbBr$_4$	20.7	80.2	Yes
(AEA)PbBr$_4$	22.4	61.1	Yes
(HIS)PbBr$_4$	22.8	59.2	Yes
(GABA)$_2$PbBr$_4$	23.9	79.6	Yes

† Abbreviations used: nBA = *n*-butylammonium, ETA = ethanolammonium, PEA = phenethylammonium, MPenDA = 2-methyl-1,5-pentanediammonium, ODA = 1,8-diammoniooctammonium, BDA = butanediammonium, AEA = ammonioethylanilinium, HIS = histammonium, GABA = 4-aminobutyric acid.

Time-resolved photoluminescence of (GABA)$_2$PbBr$_4$

The time-resolved photoluminescence data vary between samples. The decay times were calculated from time-resolved photoluminescence data using $R(t) = B_1 \exp(-t/\tau_1) + B_2 \exp(-t/\tau_2)$ and are well described by two exponential decays. The emission behavior in (GABA)$_2$PbBr$_4$ (Figure S12, Table S4) is more complex; there is single-ensemble (as the spectrum does not change as a function of decay time) and multi-ensemble behavior between samples. In Figure S12 at wavelengths 500 nm, 550 nm, and 581 nm the behavior is primarily single-ensemble-like with spectrally sensitive time scales ($\approx 49\pm18$ ns for τ_1 and $\approx 316\pm99.5$ ns for τ_2). At wavelengths $\geq$ 610 nm, the decay time is much shorter ($\tau_1 \approx 10\pm4.5$ ns and $\tau_2 \approx 201\pm82$ ns) than in the other broad wavelengths probed indicative of multi-ensemble behavior. At 77 K where time-resolved data were collected for the broad spectrum the rotational motion of GABA is extrapolated to $\approx$ 1.5 ns, this is faster than the decay times across all wavelengths. This varies from Figure 8b in the main text; where the behavior is single-ensemble like across all wavelengths. As the rotational motions

are not static when compared to decay times, one would expect time scales to be more spectrally independent as seen in the main text. The sample-dependent behavior is indicative of a surface or microstructure difference.[3] Performing spectroscopy on single crystals would eliminate the microstructure as a variable and provide a comprehensive study on the decay lifetimes of layered perovskites.

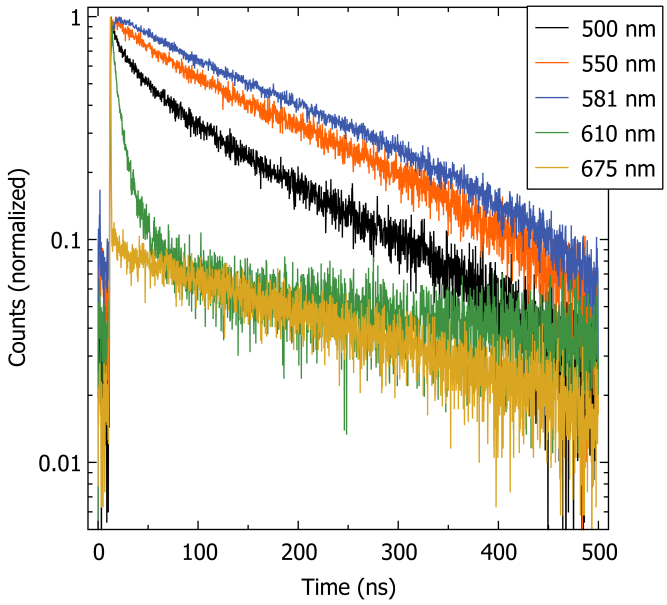

Figure S12: Time-resolved photoluminescence data for $(GABA)_2PbBr_4$. Time-resolved photoluminescence of $(GABA)_2PbBr_4$ at 500 nm (black), 550 nm (red), 581 nm (blue), 610 nm (green), and 675 nm (yellow) at 77 K. Data were normalized to the photoluminescence intensity at $\approx$ 158 ns. Decay times are listed in Table S4.

Table S4: Decay times of $(GABA)_2PbBr_4$ calculated from time-resolved photoluminescence with $R(t) = B_1 \exp(-t/\tau_1) + B_2 \exp(-t/\tau_2)$. The data are well described by a bi-exponential decay consisting of two components. τ_1 is shorter than τ_2 at all wavelengths measured. Error bars represent one standard deviation.

Decay times (ns)		
Wavelength (nm)	$\tau 1_{GABA}$	$\tau 2_{GABA}$
500	26±0.9	190±4
550	51±4	330±23
581	72±7	430±47
610	9.5±0.2	120±6
675	0.3±0.04	283±10

EISF jump models implemented in Python:

In [1]:
```
import numpy as np
from scipy.optimize import leastsq
from scipy import integrate
from scipy.optimize import curve_fit
from scipy.optimize import fsolve
```

In [2]:
```
def AY(th):
    #https://en.wikipedia.org/wiki/Rotation_formalisms_in_three_dimensions
    th = th *np.pi/180
    costh = np.cos(th)
    sinth = np.sin(th)
    M = np.array([[costh,0,sinth],[0,1,0],[-1.*sinth,0,costh]])
    return M

def AZ(ps):
    #https://en.wikipedia.org/wiki/Rotation_formalisms_in_three_dimensions
    ps = ps *np.pi/180
    cosps = np.cos(ps)
    sinps = np.sin(ps)
    M = np.array([[cosps,-1*sinps,0],[sinps,cosps,0],[0,0,1]])
    return M

def distance(a,b):
    return np.linalg.norm(a-b)
```

In [3]:
```
# Initial positions (x,y,z):
NH3rot =
[[-5.16980050e-01,  8.95568003e-01,  1.17360000e+00], #H1
 [-5.17022706e-01, -8.95539369e-01,  1.17360000e+00], #H2
 [ 1.03409857e+00,  5.55111512e-17,  1.17360000e+00], #H3
 [ 1.00862640e+00,  8.73806464e-01, -1.00101162e+00], #H4 - placeholder
 [ 1.00862640e+00, -8.73806464e-01, -1.00101162e+00]] #H5 - placeholder

def positions(Yangle,Xoffset):
    # Generate the shifted H positions based upon fitting parameters:
    NH3rot2 = np.dot(AY(Yangle),NH3rot.T).T
    NH3final = NH3rot2 - np.array([Xoffset,0,0])
    # Generate second set (positions 4-6) via C2 rotation:
    NH3_C2 = np.dot(AZ(180),NH3final.T).T
    return NH3final,NH3_C2

def distances(Yangle,Xoffset,dlib):
    NH3final,NH3_C2=positions(Yangle,Xoffset)
    # Generate jump distances for EISF calculations:
    # C2xC3 model from SI doi: 10.1063/1.5131667
    # See Table S.X.
    r0 = distance(NH3final[0],NH3final[1]) ## R1,2
    r1 = distance(NH3final[0],NH3_C2[0])   ## R1,4
    r2 = distance(NH3final[1],NH3_C2[1])   ## R2,5
    r3 = distance(NH3final[2],NH3_C2[2])   ## R3,6
    r4 = distance(NH3final[0],NH3_C2[1])   ## R1,5
    r5 = distance(NH3final[0],NH3_C2[2])   ## R1,6
    r6 = distance(NH3final[1],NH3_C2[2])   ## R2,6
    d1 = distance(NH3final[4],NH3_C2[4])   ## R7,9
    d2 = distance(NH3final[3],NH3_C2[3])   ## R8,10
    return [r0,r1,r2,r3,r4,r5,r6,d1,d2,dlib]

# Calculate EISFs based upon those structures:
j0=lambda Q,r: np.sin(Q*r)/(Q*r)

def calcEISF(Q,*params):
    # This is the full model, adapted from Lee et al.
    # See Figure S9
    Yangle = params[0]
    Xoffset = params[1]
    dlib=params[2]
    r0,r1,r2,r3,r4,r5,r6,d1,d2,dlib = distances(Yangle,Xoffset,dlib)
    # SI doi: 10.1063/1.5131667:
    # C2xC3, just describes the NH3 headgroup.
    A_A_C2xC3 = 1/18*(3+6*j0(Q,r0)+j0(Q,r1)+j0(Q,r2)+j0(Q,r3)+2*j0(Q,r4)+2*j0(Q,r5)
+2*j0(Q,r6))
    # C2XE for CH2 adjacent to NH3 terminal group.
    A_A_C2xE = 1/4*(2 + j0(Q,d1) + j0(Q,d2))
    # Libration for CH2 groups:
    A_A_C2lib = 1/8 * (4+4*j0(Q,dlib))
    # Methyl rotation:
    A_A_C3 = 1/9 * (3+6*j0(Q,r0))
    A_total = (3*A_A_C2xC3 + 2*A_A_C2xE + 4*A_A_C2lib + 3*A_A_C3)/12
    return A_total

def calcEISF_C3lib(Q,dlib):
    # This is just C3 motion of the -CH3 and -NH3 ends with libration
    r0 = distance(NH3rot[0],NH3rot[1])
    A_A_C3 = 1/9 * (3+6*j0(Q,r0))
```

```
    # Libration for 6 CH2 groups:
    A_A_C2lib = 1/12 * (6+6*j0(Q,dlib))
    A_total = (6*A_A_C3 + 6*A_A_C2lib)/12
    return A_total

def calcEISF_C3(Q):
    # This is just C3 motion of the -CH3 and -NH3 ends
    # See Figure S10
    r0 = distance(NH3rot[0],NH3rot[1])
    A_A_C3 = 1/9 * (3+6*j0(Q,r0))
    static = np.ones(np.shape(Q))
    A_total = (6*A_A_C3 + 6*static)/12
    return A_total

def calcEISF_C3_variablefrac(Q,frac):
    # This is just C3 motion of the -CH3 and -NH3 ends with variable fraction of mo
tion
    # See Figure S11, Table S2
    r0 = distance(NH3rot[0],NH3rot[1])
    A_A_C3 = 1/9 * (3+6*j0(Q,r0))
    static = np.ones(np.shape(Q))
    A_total = (6*frac*A_A_C3 + 6*(2-frac)*static)/12
    return A_total

def calcEISFs(Q,*params):
    # This is the full motion of the Lee model, but we return all of the different
 contributions
    # See Figure S9
    Yangle = params[0]
    Xoffset = params[1]
    dlib=params[2]
    r0,r1,r2,r3,r4,r5,r6,d1,d2,dlib = distances(Yangle,Xoffset,dlib)
    # SI doi: 10.1063/1.5131667:
    # C2xC3, just describes the CH2NH3 headgroup
    A_A_C2xC3 = 1/18*(3+6*j0(Q,r0)+j0(Q,r1)+j0(Q,r2)+j0(Q,r3)+2*j0(Q,r4)+2*j0(Q,r5)
+2*j0(Q,r6))
    # C2XE for CH2 adjacent to NH3 terminal group
    A_A_C2xE = 1/4*(2 + j0(Q,d1) + j0(Q,d2))
    # Libration for CH2 groups
    A_A_C2lib = 1/8 * (4+4*j0(Q,dlib))
    # Methyl rotation
    A_A_C3 = 1/9 * (3+6*j0(Q,r0))
    A_total = (3*A_A_C2xC3 + 2*A_A_C2xE + 4*A_A_C2lib + 3*A_A_C3)/12
    return A_total,3/12*A_A_C2xC3,2/12*A_A_C2xE ,4/12*A_A_C2lib,3/12*A_A_C3
```

References

(1) Smith, M. D.; Jaffe, A.; Dohner, E. R.; Lindenberg, A. M.; Karunadasa, H. I. Structural origins of broadband emission from layered Pb-Br hybrid perovskites. *Chemical Science* **2017**, *8*, 4497–4504.

(2) Hu, X.; Zhang, D.; Chen, T.; Chen, A. Z.; Holmgren, E. N.; Zhang, Q.; Pajerowski, D. M.; Yoon, M.; Xu, G.; Choi, J. J.; Lee, S.-H. Crystal structures and rotational dynamics of a two-dimensional metal halide perovskite $(OA)_2PbI_4$. *The Journal of Chemical Physics* **2020**, *152*, 014703.

(3) Thomaz, J. E.; Lindquist, K. P.; Karunadasa, H. I.; Fayer, M. D. Single Ensemble Non-exponential Photoluminescent Population Decays from a Broadband White-Light-Emitting Perovskite. *Journal of the American Chemical Society* **2020**, *142*, 1662216631.